

# AIPL1, a Protein Associated with Childhood Blindness, Interacts with $\alpha$ -Subunit of Rod Phosphodiesterase (PDE6) and Is Essential for Its Proper Assembly\*

Received for publication, June 23, 2009, and in revised form, September 11, 2009. Published, JBC Papers in Press, September 16, 2009, DOI 10.1074/jbc.M109.036780

Saravanan Kolandaivelu<sup>‡</sup>, Jing Huang<sup>§</sup>, James B. Hurley<sup>§</sup>, and Visvanathan Ramamurthy<sup>‡1</sup>

From the <sup>‡</sup>Departments of Ophthalmology and Biochemistry, Sensory Neuroscience Research Center, West Virginia University, Morgantown, West Virginia 26506 and the <sup>§</sup>Departments of Biochemistry and Ophthalmology, University of Washington, Seattle, Washington 98195

Mutations in the gene coding for AIPL1 cause Leber congenital amaurosis (LCA), a severe form of childhood blindness. The severity in disease is reflected in the complete loss of vision and rapid photoreceptor degeneration in the retinas of mice deficient in AIPL1. Our previous observations suggest that rod photoreceptor degeneration in retinas lacking AIPL1 is due to the massive reduction in levels of rod cGMP phosphodiesterase (PDE6) subunits ( $\alpha$ ,  $\beta$ , and  $\gamma$ ). To date, the crucial link between AIPL1 and the stability of PDE6 subunits is not known. In this study using *ex vivo* pulse label analysis, we demonstrate that AIPL1 is not involved in the synthesis of PDE6 subunits. However, *ex vivo* pulse-chase analysis clearly shows that in the absence of AIPL1, rod PDE6 subunits are rapidly degraded by proteasomes. We further demonstrate that this rapid degradation of PDE6 is due to the essential role of AIPL1 in the proper assembly of synthesized individual PDE6 subunits. In addition, using a novel monoclonal antibody generated against AIPL1, we show that the catalytic subunit ( $\alpha$ ) of PDE6 associates with AIPL1 in retinal extracts. Our studies establish that AIPL1 interacts with the catalytic subunit ( $\alpha$ ) of PDE6 and is needed for the proper assembly of functional rod PDE6 subunits.

Leber congenital amaurosis (LCA)<sup>2</sup> is an early childhood blinding disease that affects the retina. At a very young age, children affected with LCA lack both scotopic and photopic visual response implying both rod and cone photoreceptors dysfunction (1). To date, mutations in 14 genes, including the *Aipl1* gene have been linked to this disease (1, 2). A recent study showed that an adult LCA patient with a mutation in *Aipl1* has

no visual response (3). In addition, immunohistochemistry using rod markers showed that the patient had no rod photoreceptors. Although some remnants of cone photoreceptors remained, the outer segments were completely missing, suggesting a degeneration of both rod and cone photoreceptors in this LCA patient.

AIPL1 is specifically expressed in retina and in the pineal gland. In retina, AIPL1 is expressed in young and adult rod photoreceptors (4, 5). However, AIPL1 is expressed in cones transiently and is thought to be absent from adult cones (3). Two independent studies demonstrated that mice lacking AIPL1 undergo a rapid and severe retinal degeneration with both rod and cone photoreceptor loss (6, 7). Although AIPL1 was not essential for the initial formation of photoreceptor cells, the photoreceptor cells were not functional, as they could not evoke any light-dependent electrical response (6). These results are consistent with the disease characteristics of LCA (8). Our previous studies show that before degeneration, rod PDE6 activity and the levels of PDE6 protein are drastically reduced in the absence of AIPL1 (6). In addition to the knockout mouse, an AIPL1 knockdown mouse was created in which AIPL1 expression was reduced to 20–25% of wild-type levels (9). The knockdown mouse showed normal development and retinal morphology up to 3 months of age. At 3 months, the rod photoreceptor outer segments become disorganized, and by 8 months, more than half of the photoreceptors are lost. A reduction in rod PDE6 was also observed in the AIPL1 knockdown mouse. In contrast to *Aipl1*<sup>-/-</sup> mice, cones are not affected in the AIPL1 knockdown mouse up to 11 months (6, 9). These results demonstrate that AIPL1 plays a vital role in the maintenance and functioning of rod photoreceptor cells by affecting the rod PDE6 levels. However, the role of AIPL1 in cones is still not clear.

PDE6 is a critical enzyme expressed in retina and is needed to convert visual light stimuli into electrical signals in photoreceptor cells (10). Light stimulates phototransduction by activating PDE6 to hydrolyze cyclic GMP. Rod and cone photoreceptors contain separate but related PDE6 subunits. Rod PDE6 is composed of two homologous catalytic subunits ( $\alpha$  and  $\beta$ ) and two copies of an inhibitory ( $\gamma$ ) subunit (11–16). The biosynthesis of functional PDE6 heterotetramer involves complex post-transcriptional processing that includes prenylation of PDE6 catalytic subunits, assembly of the three subunits of PDE6, and further transport of these subunits from inner to outer segments of

\* This work was supported, in whole or in part, by National Institutes of Health Grant EY017035 from the NEI (to V. R.) and COBRE Grant P20 RR15574 (to the Sensory Neuroscience Research Center). This work was also supported by a Research to Prevent Blindness Challenge grant (to West Virginia University), the International and West Virginia Lions Eye Foundation (to West Virginia University) and a Knight Templar Eye Foundation grant (to S. K.), and Vision Core Grant P30EY1730 (to University of Washington).

<sup>1</sup> To whom correspondence should be addressed: Dept. of Ophthalmology, WV University Eye Institute, One Stadium Dr., P. O. Box 9193, Morgantown, WV 26506-9193. Tel.: 304-598-4893; Fax: 304-598-6928; E-mail: ramamurthyv@wvuuh.com.

<sup>2</sup> The abbreviations used are: LCA, Leber congenital amaurosis; AIPL1, aryl hydrocarbon receptor interacting protein like 1; IRBP, interphotoreceptor retinoid-binding protein; DMEM, Dulbecco's modified Eagle's medium; IP, immunoprecipitation; PN, postnatal; PDE6, cGMP phosphodiesterase type 6; *rd*, retinal degeneration mouse; *Nrl*, neural retina leucine zipper transcription factor; mAb, monoclonal antibody; ROS, rod outer segment.

## AIPL1 and PDE6 Stability

photoreceptors. It is not clear if prenylation precedes the assembly of PDE6 subunits and if assembly of PDE6 subunits is required for their transport to outer segments. Mutations or alteration in any one of the subunits ( $\alpha$ ,  $\beta$ , and  $\gamma$ ) cause rapid photoreceptor degeneration and retinitis pigmentosa (17–19). Both PDE6  $\beta$  and PDE6  $\gamma$  are required for activity but not for the stability of the remaining subunits in the retina before the onset of retinal degeneration (19). Retinas lacking AIPL1 show the same type of rapid degeneration observed in photoreceptors lacking in PDE6  $\beta$  or PDE6  $\gamma$ . In contrast to other mouse models, all three subunits of rod PDE6 are drastically destabilized (reduced by 90%) before the onset of retinal degeneration in retinas lacking AIPL1 (6). The mRNA levels of PDE6 subunits are not altered in *Aipl1*<sup>-/-</sup> retinas (6). These observations suggest that AIPL1 affects post-transcriptional processing of PDE6 subunits and is crucial for early steps of biosynthesis of PDE6 subunits.

The connection between AIPL1 and rod PDE6 stability has not yet been identified. This study explores the link between AIPL1 and stability of PDE6 subunits. Our study also demonstrates an interaction between AIPL1 and the  $\alpha$ -subunit of PDE6.

### EXPERIMENTAL PROCEDURES

**Materials**—Cell culture reagents and secondary antibodies were purchased from Invitrogen. FuGENE 6 transfection reagent and protease inhibitor mixture tablets were purchased from Roche Diagnostics. The phosphatase inhibitor mixture set, MG132, leucinal, and lactacystin are from Calbiochem (Gibbstown, NJ). [<sup>35</sup>S]Methionine was purchased from GE Healthcare. Supplies for immunoblotting were from Millipore (Billerica, MA). Leupeptin, pepstatin, soybean trypsin inhibitors, aprotinin, and all other chemicals were obtained from Sigma or Fisher.

**Antibodies**—Polyclonal antiserum to the AIPL1 protein was affinity purified on a glutathione *S*-transferase-AIPL1 column (FL antibody) as described earlier (22). Commercial antibodies to other proteins included rod PDE6  $\alpha$  and  $\beta$  antibodies (Affinity BioReagents, Golden, CO), and MOE rabbit polyclonal antibody against PDE6  $\alpha$ ,  $\beta$ , and  $\gamma$  subunits (Cytosignal Inc., Irvine, CA). Antibodies to PDE6 subunits (ROS-1) and PDE6  $\gamma$  inhibitory subunits (R4842) were generously provided by Drs. Ted Wensel (Baylor College) and Joe Beavo (University of Washington). Rod arrestin antibody was a gift from Dr. Cheryl Craft, University of California, Los Angeles.

**cDNA Cloning**—The cDNA containing the coding region of mouse rod PDE6  $\alpha$  and rod PDE6  $\beta$  were generated by PCR using forward primers 5'-AGTCTTCACCATGGGTGAGGTG-3' (mouse rod PDE  $\alpha$ ) and 5'-ATGAGCAGTGGGGAA-CAGGTAC-3' (mouse PDE  $\beta$ ), and reverse primers 5'-GTCA-GCTACTGGATGCAACAGGACT-3' (mouse rod PDE  $\alpha$ ) and 5'-ACACGGCTTATAGGATACAGCAGGT-3' (mouse PDE  $\beta$ ). These primers were designed based on the cDNA sequences of mouse PDE  $\alpha$  (BC044892) and mouse PDE  $\beta$  (BC129923). For these PCR, we used retinal cDNA as template. Briefly, mouse retinal cDNAs were prepared from total RNA of adult C57bl/6 mouse retinal tissue using TRIzol (Invitrogen) reagent followed by reverse transcription using the SuperScript III one-

step RT-PCR system (Invitrogen). Oligo(dT) primer was used to generate cDNA. PCR was performed with Pfu-ultra fusion DNA polymerase (Stratagene, La Jolla, CA) at a denaturing temperature of 95 °C for 30 s, followed by annealing at 58 °C for 30 s, and extension at 72 °C for 2 min (35 cycles). The resultant PCR products were digested with restriction enzymes and subcloned into eukaryotic expression vector pTriEx-4 (Novagen, Madison, WI). To make sure that there are no errors, all constructs were sequenced in both directions.

**SDS-PAGE and Immunoblotting**—Two dissected retinas were homogenized in 100  $\mu$ l of ROS buffer (20 mM Hepes, pH 7.4, 60 mM KCl, 2 mM MgCl<sub>2</sub>, 30 mM NaCl, 100  $\mu$ M phenylmethylsulfonyl fluoride, 1 mM dithiothreitol, 5 mM 2-mercaptoethanol) and protease inhibitors (Roche Diagnostics) using a pellet pestle (VWR, West Chester, PA) in a 1.5-ml Eppendorf tube on ice. Homogenization was repeated for three pulses (15 s  $\times$  3). Homogenized extracts were solubilized by adding an equal volume of 2 $\times$  SDS loading buffer (Bio-Rad) followed by heating the samples at 100 °C for 5 min. Equal amounts (50  $\mu$ g) of sample were separated by SDS-PAGE, transferred to Immobilon-FL membrane (Millipore), and probed with antibodies. Total protein concentration was estimated by BCA assay before addition of SDS loading buffer (Bio-Rad).

**Pulse Labeling and Immunoprecipitation**—Mice were sacrificed on postnatal day 8 (PN day 8), eyes were enucleated, and the retinas were collected. Four retinas were incubated in 400  $\mu$ l of Dulbecco's modified Eagle's medium (DMEM) lacking *dl*-methionine (Invitrogen) for 30 min at 37 °C in a 95% O<sub>2</sub>, 5% CO<sub>2</sub> incubator in a 24-well tissue culture plate. To reduce the variability among various samples we combined 4 retinas from 2 different mice. After methionine depletion, retinas were transferred in 400  $\mu$ l of DMEM containing L-[<sup>35</sup>S]methionine (1 mCi/mmol, GE Healthcare) for the indicated times. For the pulse-chase, radioactive *dl*-methionine incorporation was performed for 1½ h followed by two washes (500  $\mu$ l) in DMEM and further incubated in fresh DMEM supplemented with 500  $\mu$ M cold L-methionine. At appropriate times for pulse label (0.5, 1, 1.5, and 2 h) and pulse-chase (0, 1, and 3 h), retinas were removed and immediately frozen at -80 °C on dry ice to prevent further incorporation of label and protein degradation.

Frozen retinas (4) were homogenized in 400  $\mu$ l of 1 $\times$  phosphate-buffered saline containing protease inhibitors and 1 mM iodoacetamide using a pellet pestle (VWR) in a 1.5-ml Eppendorf tube on ice (15 s  $\times$  3). After homogenization, Triton X-100 was added to a final concentration of 0.5% Triton X-100 (total volume: 800  $\mu$ l). The homogenized retinal extracts were pre-cleared by addition of 20  $\mu$ l of immunopure immobilized protein A plus beads (Fisher) by incubating at 4 °C for 1 h. Supernatants were collected by centrifuging at 10,000  $\times$  g (Eppendorf 5424) for 5 min at 4 °C. Immunoprecipitation was carried out with supernatants (400  $\mu$ l) using the indicated antibodies (20).

For immunoprecipitations (IP), we used 2.5  $\mu$ l of MOE antiserum (0.072 mg) or 1.5  $\mu$ g of ROS-1 monoclonal antibody for each pulldown experiment. Proteins were either separated by 4–20% SDS-polyacrylamide gel (Bio-Rad) or by a special gel (containing 0.15% bisacrylamide) to separate the rod PDE6  $\alpha$  and PDE6  $\beta$  subunits. For detection of radioactive samples, the gels were impregnated with a fluorography enhancer as

described by manufacturer (Amplify, GE Healthcare), dried, and exposed to autoradiography on Biomax MR film (Kodak) for 3–7 days at  $-80^{\circ}\text{C}$ .

For experiments analyzing stability of PDE6 in the presence of proteasomal inhibitors, after 2 h of pulse labeling of retina, 10  $\mu\text{M}$  each of lactacystin, leucinal, and MG132 was added and then pulse-chase was performed for 3 h. As a control, we analyzed the stability of PDE6 in the presence of DMSO, a solvent used to solubilize the inhibitors.

**Overexpression of Recombinant Rod PDE6  $\alpha$  and PDE6  $\beta$  Subunits Using COS-7 Cells**—COS-7 cells were grown at  $37^{\circ}\text{C}$  to 70% confluence in a 100-mm dish containing DMEM with 10% fetal bovine serum in a humidified 5%  $\text{CO}_2$  and 95% air incubator. After 24 h of plating, the cells were then transfected with 2  $\mu\text{g}$  of plasmids using FuGENE transfection reagent (Roche). After 48 h of growth, the cells were harvested by adding 750  $\mu\text{l}$  of Hanks balanced salt solution with 1 mM EDTA at room temperature for 3 min. The cells were pelleted down by centrifuging at  $8000 \times g$  for 2 min (Eppendorf 5424) and re-suspended in 200  $\mu\text{l}$  of  $1 \times$  phosphate-buffered saline containing protease inhibitors and benzonase (Novagen). The re-suspended cells were sonicated for 5 pulses for 3 s each on ice (Microson XL2000 Ultrasonic cell disruptor; VWR). The homogenates were solubilized with  $2 \times$  SDS loading buffer (Bio-Rad) and boiled before loading on SDS-PAGE gel.

For labeling experiments, after 48 h of transfection, medium was switched to DMEM lacking methionine for 6 h followed by DMEM containing  $L$ - $[^{35}\text{S}]$ methionine (1 mCi/mmol, GE Healthcare) for 24 h. Cells were collected, homogenized by sonication, and immunoprecipitation was performed as described earlier.

**Creation of Monoclonal Antibody against AIPL1**—Full-length cDNA encoding AIPL1 was amplified from mouse retinal cDNA, and cloned in fusion with C-terminal His<sub>6</sub> tags in pTriEX-4 (Novagen, Madison, WI) plasmid. His-tagged mAIP1 was purified from a soluble fraction of *Escherichia coli* extracts using the His tag purification kit (Novagen). Purified recombinant mAIP1 protein was used to immunize BALB/c mice. Hybridomas were generated by fusion of BALB/c parental myeloma cells with splenocytes from the immunized mice according to the procedure described by Campbell (38). Supernatants from the hybridomas were screened by enzyme-linked immunosorbent assay. The positive clones were further screened by immunocytochemistry and immunoprecipitation subsequent to cloning by limiting dilution. Eight positive clones were selected from subclones and clone mAb-AIPL1 was used for further ascites production. Large scale ascites productions were done commercially (Maine Biotechnology Service, Inc., Portland, ME). Further purification of antibody was performed using the melon gel purification kit (Pierce) according to the instructions from the manufacturer.

**Bovine Retinal Extracts Preparation**—Two frozen bovine retinas (InVision BioResources, Seattle, WA) were homogenized with 6 ml of buffer A containing 10 mM Tris-HCl (pH 7.5), 100 mM KCl, 20 mM NaCl, 1 mM EDTA, 1 mM  $\text{MgCl}_2$ , 10 mM iodoacetamide, with protease and phosphatase inhibitors (1 protease inhibitor mini-tablet for 6 ml of buffer, 2  $\mu\text{g}/\text{ml}$  of leupeptin and pepstatin, 6  $\mu\text{l}$  of phosphatase inhibitor mixture, and 25  $\mu\text{g}/\text{ml}$

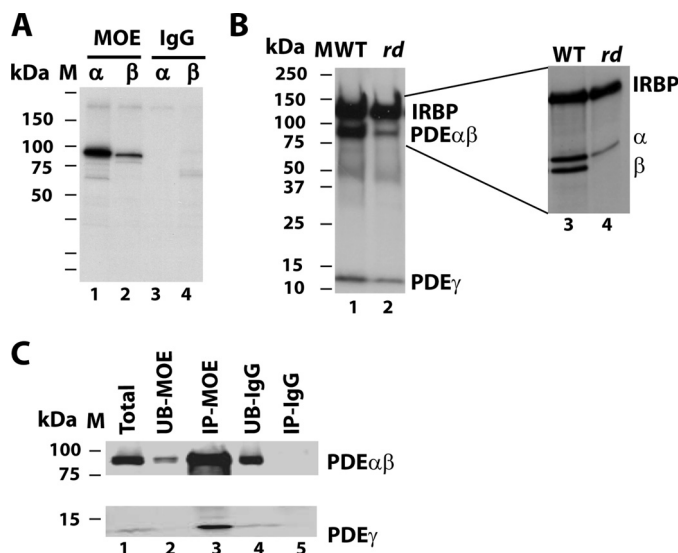


**FIGURE 1. MOE antibody recognizes individual unassembled PDE6 subunits.** A, MOE antibody immunoprecipitates individually expressed and radioactively labeled PDE6  $\alpha$  and PDE6  $\beta$  subunits in COS cells (lanes 1 and 2). As a control, nonspecific rabbit IgGs do not recognize PDE6 subunits (lanes 3 and 4). UB, unbound fraction. B, MOE antibody immunoprecipitates all three subunits ( $\alpha$ ,  $\beta$ , and  $\gamma$ ) in PN day 8 wild-type (+/+) retinal extracts (lanes 1 and 3). It also recognizes unassembled PDE6  $\alpha$  and  $\gamma$  in retinas from PN day 8 rd retinal extracts (lanes 2 and 4). A 0.15% bisacrylamide gel that results in better separation of PDE6  $\alpha$  and  $\beta$  subunits clearly shows that the PDE6  $\beta$  subunit is missing in retinas from rd mice (lane 4). IRBP serves as a control protein and co-immunoprecipitates with PDE6 subunits. C, MOE antibody immunoprecipitates the majority (95%) of PDE6 ( $\alpha$ ,  $\beta$ , and  $\gamma$ ) from PN day 8 wild-type retinal extracts (compare lane 1 with 2). As a control, nonspecific rabbit IgGs do not recognize PDE6 subunits (lanes 1 and 4). Note: in all IP experiments relative to extracts, IP samples are concentrated ( $\times 10$ ), as they were eluted in a smaller volume.

of soybean trypsin inhibitor). Retinal tissue were homogenized using a glass/Teflon homogenizer (10–12 strokes), and centrifuged at  $10,000 \times g$  for 5 min (Eppendorf centrifuge 5424). Supernatants were further centrifuged at high speed at  $50,000 \times g$  for 30 min at  $4^{\circ}\text{C}$  (Beckman Optima TLX ultracentrifuge TLA-55R). This high speed supernatant was then used for IP, similar to the method described above.

**Gel Filtration**—Twenty retinas from wild-type and mice lacking AIPL1 were homogenized, as described for the bovine retinal extract preparation, with buffer B (50 mM Tris-HCl, pH 7.5, 0.2 mM  $\text{MgCl}_2$ , and 1 mM dithiothreitol with protease and phosphatase inhibitors) to extract PDE6 complex. Extraction with hypotonic buffer was repeated twice and the supernatants containing PDE6 were combined together. Western blot analysis using a PDE6 antibody confirmed that the majority of PDE6 was extracted by buffer B. A Superdex-200 10/300 GL gel filtration column (Amersham Biosciences), equilibrated with buffer B was used for separating the protein complex. The sample (0.5 ml) was applied to an equilibrated column at a constant flow rate of 0.5 ml/min. Eluted fractions were further analyzed by Western blotting to determine the migration of PDE6 ( $\alpha$ ,  $\beta$ , and  $\gamma$ ) subunits. The gel filtration column was calibrated with the following standards: thyroglobulin (670 kDa),  $\gamma$ -globulin (158 kDa), ovalbumin (44 kDa), myoglobin (17 kDa), and vitamin B<sub>12</sub> (1.355 kDa).

## RESULTS

**AIPL1 Does Not Affect the Synthesis (Translation) of PDE6 Message**—Mouse models with deficiency in AIPL1 suggest that it plays a crucial role in the post-transcriptional processing of

## AIPL1 and PDE6 Stability

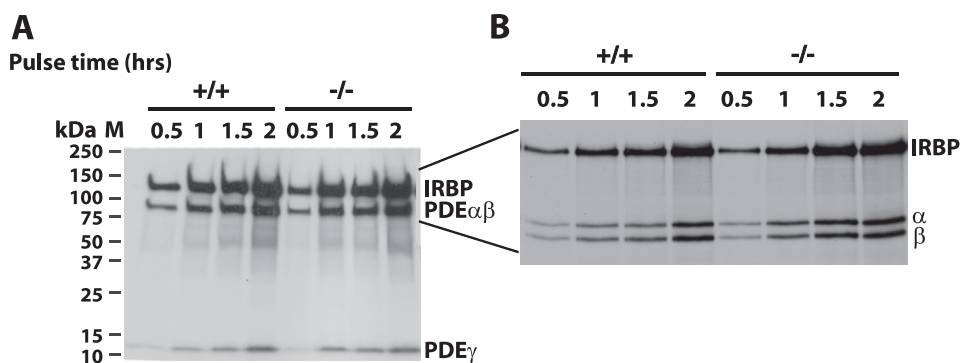


**FIGURE 2. AIPL1 is not needed for synthesis of PDE6 subunits.** Protein synthesis was monitored in retinas from PN day 8 wild-type (+/+) or mice lacking AIPL1 (-/-). Following depletion of methionine for 30 min, retinas were incubated in medium containing radioactive L-[<sup>35</sup>S]methionine for the indicated amount of time. The amount of PDE6 synthesized was measured by immunoprecipitation using MOE antibody followed by fluorography. *A*, the initial rate of PDE6  $\alpha$ ,  $\beta$ , and  $\gamma$  subunits until 2 h of labeling is not affected by the absence of AIPL1. *B*, a 0.15% bisacrylamide gel that results in better separation of PDE6  $\alpha$  and  $\beta$  subunits shows a similar result. Each experiment was repeated at least three times with similar results.

PDE6 (6, 9, 21). Because, AIPL1 protein primarily resides within photoreceptor inner segments, the putative role of AIPL1 must be restricted to its influence on post-transcriptional processing of PDE6 within the inner segments (22, 23). These processes include synthesis, folding, assembly, and prenylation of the PDE6 heterotetramer.

To investigate the role of AIPL1 in translation of the PDE6 message, we monitored the synthesis of PDE6 subunits at PN day 8 in retina from wild-type mice and from mice lacking AIPL1. We chose retina from the PN day 8 stage because our previous studies using electron microscopy showed that there were no discernible changes in the morphology of retina due to lack of AIPL1 (6). In addition, radiolabel incorporation of methionine in retinal proteins was much better at PN day 8 (data not shown). We initially compared protein synthesis from eyecups or retina in culture. In our hands, eyecups fall apart in culture medium after 6 h (data not shown). Therefore, we decided to monitor protein synthesis in the retina. Isolated retinas were incubated in medium (prewarmed at 37 °C) lacking methionine for 30 min to deplete the endogenous methionine. For each time point, we combined four retinas from two different mice to avoid large variations. To label the newly synthesized proteins, retinas were transferred to medium containing L-[<sup>35</sup>S]methionine for 30 min to 2 h. At the indicated times, retinas were collected and quickly frozen in dry ice. Overall protein synthesis, as measured by radioactivity incorporated in trichloroacetic acid-precipitable proteins, was similar between retinas from wild-type and from the mice lacking *Aipl1* (data not shown). The levels of newly synthesized PDE6 subunits were analyzed by immunoprecipitating all three rod PDE6 subunits using a polyclonal PDE6 antibody (MOE). Immunoprecipitates were further analyzed by SDS-PAGE followed by fluorography to detect the radiolabeled PDE6 subunits.

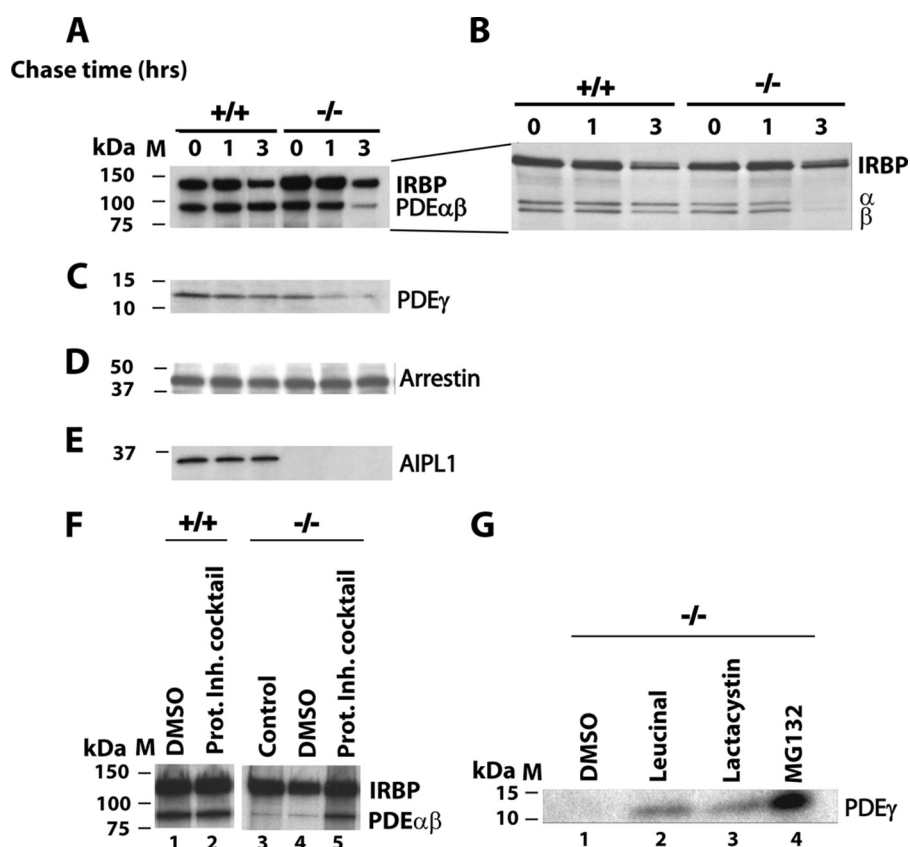


**FIGURE 3. PDE6 subunits are unstable in the absence of AIPL1.** Pulse-chase experiments were performed with retinas in culture from PN day 8 wild-type (+/+) or mice lacking AIPL1 (-/-). After 1½ h of radioactive labeling, pulse-chase was initiated by addition of media containing excess cold methionine for the indicated amounts of chase time. PDE6  $\alpha$ ,  $\beta$ , and  $\gamma$  subunits are stable up to 3 h in wild-type retina (*A* and *B*). In contrast, PDE6  $\alpha$ ,  $\beta$ , and  $\gamma$  subunits are highly sensitive to proteolytic degradation and the majority of PDE6 subunits degrade within 3 h of chase (*A*–*C*). The stability of individual PDE6  $\alpha$  and  $\beta$  subunits are affected as seen by a special 0.15% bisacrylamide gel to separate the PDE6  $\alpha$  and  $\beta$  subunits (*B*). As a control, we monitored the stability of rod arrestin (*D*). The stability of AIPL1 was monitored in wild-type retinal extracts (*E*). As expected, AIPL1 is not present in retinal extracts from the knockout mice (*E*). In the presence of the proteasomal inhibitor mixture, the degradation of PDE6 in AIPL1-deficient mice was significantly reduced after 3 h of pulse-chase (*F*, compare lanes 3–5). As a control, in wild-type retina, the stability of PDE6 was not affected by the presence of inhibitor (*F*, compare lanes 1 and 2). Among the proteasomal inhibitors tested, MG132 showed an enhanced ability to prevent degradation of the PDE6  $\gamma$  subunit in the absence of AIPL1 (*G*, lanes 1–4). *DMSO*, the solvent used for solubilizing inhibitors does not alter the stability of PDE6 subunits (*F* and *G*). The images shown are representative of three independent experiments.

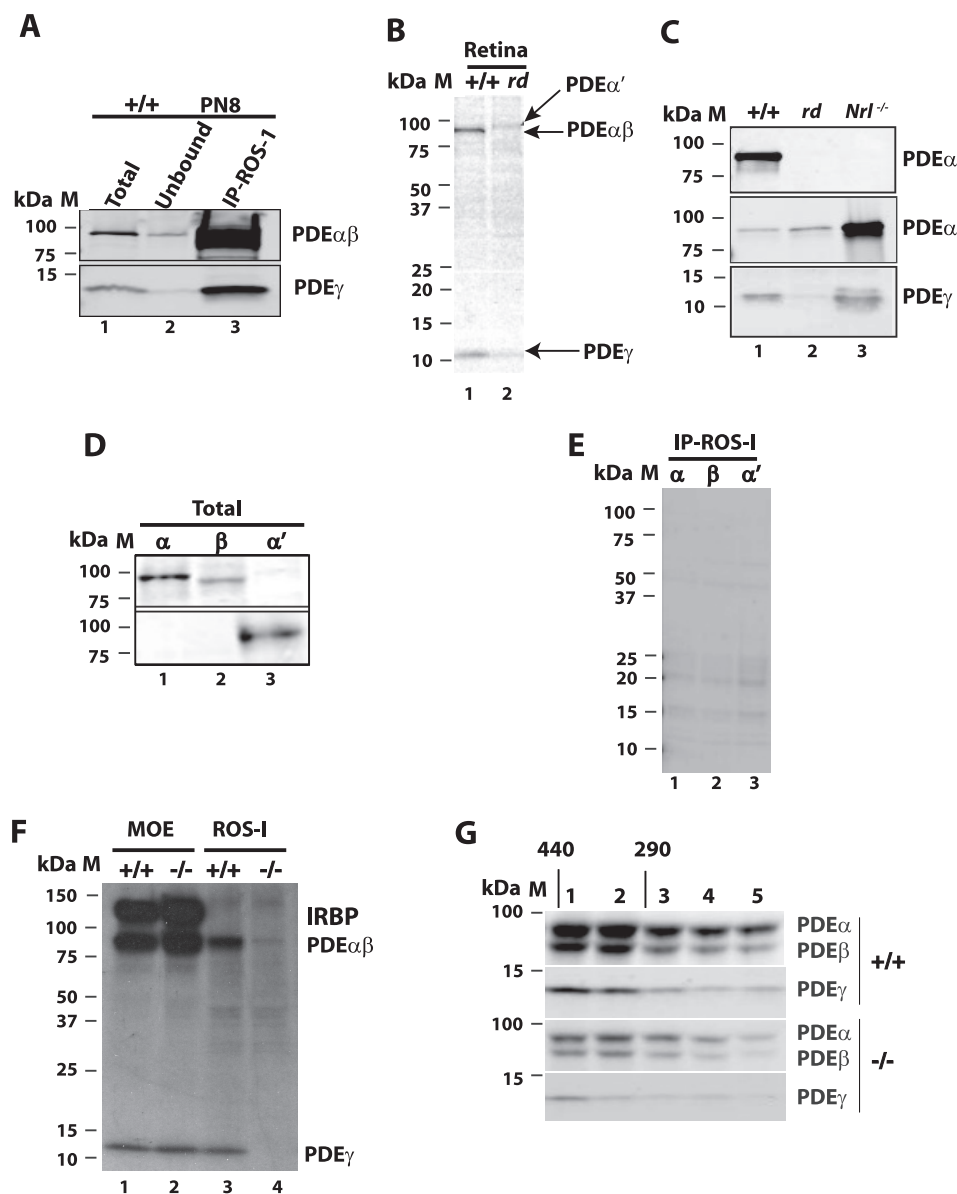


**FIGURE 4. AIPL1 is essential for proper assembly of PDE6 subunits.** *A*, ROS-1 antibody IP (lane 3) of the majority (90%) of assembled PDE6  $\alpha$ ,  $\beta$ , and  $\gamma$  subunits present in PN day 8 retinas from wild-type mice (compare lanes 1 and 2). *B*, however, in *rd* mice lacking rod PDE6  $\beta$  subunit (PN day 8), ROS-1 does not IP rod PDE subunits (lane 2). Cone PDE  $\alpha'$  present in *rd* mice is still recognized by ROS-1. *C*, IP analysis followed by Western blotting with the indicated antibody to confirm the absence of rod PDE6 pull-down by ROS-1 in *rd* mice. Assembled cone PDE  $\alpha'$  present in *rd* and cone-rich *Nrl* mice is recognized by ROS-1 (middle panel). In contrast to wild-type (+/+), ROS-1 does not recognize rod PDE6 in *rd* mice (upper panel). *D*, Western blot analysis shows the expression of individual PDE6 subunits in COS-7 cells. Top panel shows the expression of rod PDE6 catalytic subunits using MOE antibody, and the bottom panel shows the expression of cone PDE6 subunit using a cone PDE-specific antibody. *E*, ROS-1 antibody does not pull down individually expressed PDE6 subunits in COS-7 cells (lanes 1–3). *F*, ROS-1 antibody recognizes assembled PDE6 subunits from PN day 8 wild-type mice (lane 3). Although PDE6 subunits are present in retina lacking AIPL1 (PN day 8), they are not recognized by ROS-1 antibody (compare lanes 2 and 4). Identical results were observed during three independent experiments. *G*, size exclusion chromatography followed by Western blotting with MOE antibody show that all three subunits of the PDE6 enzyme elute in similar fractions in both wild-type and AIPL1-deficient mice (lanes 1–5).

Characterization of the MOE antibody shows that this antibody can precipitate unassembled, individual PDE6 subunits expressed in tissue culture cells (Fig. 1A). This is further substantiated by our results showing that MOE can precipitate PDE6 subunits from retinal degeneration (*rd*) mice retinal extracts, where the PDE6  $\beta$  subunit is missing (Fig. 1B). In addition, MOE antibody was efficient in depleting the majority (95%) of PDE present in retinal extracts (Fig. 1C). A nonspecific

protein that consistently co-precipitates at 140 kDa was identified as interphotoreceptor retinoid-binding protein (IRBP) by light chromatography-mass spectrometry (Protea Biosciences, Morgantown, WV). IRBP serves as an excellent internal control for our pulse label and chase analysis (Fig. 1B). Using the MOE antibody to measure PDE6 levels, we did not observe any significant difference in the synthesis of PDE  $\alpha$ ,  $\beta$ , and  $\gamma$  subunits in the absence of AIPL1 (Fig. 2A). Furthermore, using a special 0.15% bisacrylamide gel, which can be used to separate the comigrating PDE  $\alpha$  and  $\beta$  subunits, we demonstrate that synthesis of individual PDE  $\alpha$  or PDE  $\beta$  subunits are not affected by the lack of AIPL1 (Fig. 2B).

#### *AIPL1 Is Needed for the Stability of Nascent Rod PDE6 Polypeptides—*

To examine the influence of AIPL1 on PDE6 turnover, we performed pulse-chase experiments using retina isolated from wild-type and AIPL1-deficient mice at PN day 8. Briefly, after pulse labeling with L-[<sup>35</sup>S]methionine for an 1½ h, pulse-chase was performed by incubating the retina in medium containing cold methionine for 0, 1, and 3 h. The stability of the synthesized PDE6 subunits was measured by immunoprecipitating all three PDE6 subunits using MOE. Our results clearly show that in contrast to PDE6 subunits from wild-type retina, all three PDE6 subunits from *Aipl1*<sup>-/-</sup> retina are not stable after a 3-h pulse-chase (Fig. 3, A and C). This experiment was repeated three independent times with identical results. In contrast, rod arrestin is stable for the entire chase time in both wild-type and in retinas lacking AIPL1 (Fig. 3D). IRBP serves as an internal control and its stability is not affected by the lack of AIPL1

(Fig. 3, A and B). We also confirmed the lack of AIPL1 in retina from *Aipl1*<sup>-/-</sup> mice (Fig. 3E).

The instability of PDE6 subunits in the absence of AIPL1 can be ameliorated by addition of a proteasomal inhibitor mixture containing 10  $\mu$ M each of leucinal, lactacystin, and MG132 before initiation of the pulse-chase (Fig. 3F). Among these inhibitors, MG132 seems to stabilize the  $\gamma$  subunit of PDE6 more efficiently (Fig. 3G). Altogether, our pulse-chase analysis

## AIPL1 and PDE6 Stability

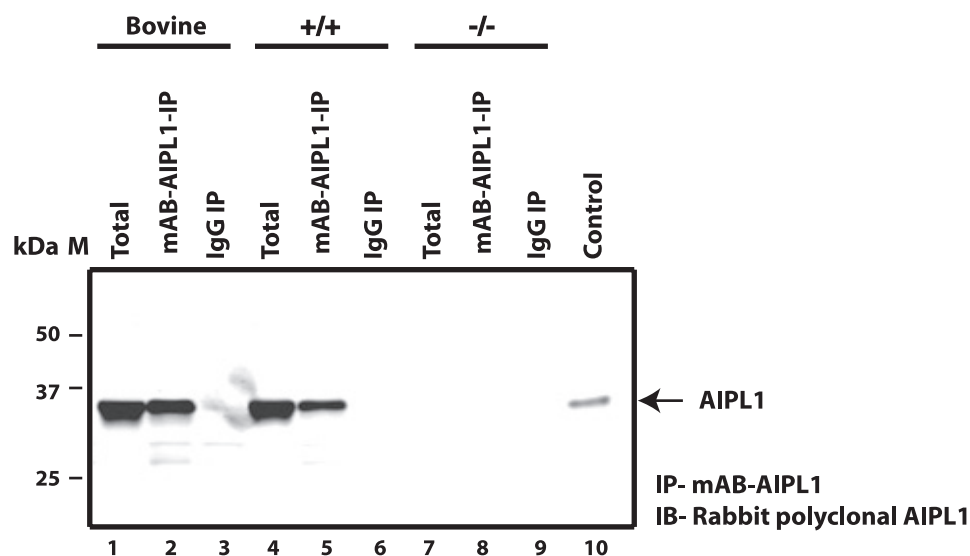


**FIGURE 5. mAb-AIPL1 recognizes native AIPL1 from retinal tissues.** IP of AIPL1 from bovine and mouse retinal extracts using mAb-AIPL1 antibody followed by Western blot with polyclonal rabbit AIPL1 antibody. mAb-AIPL1 antibody specifically pulls down AIPL1 from bovine retinal extracts (compare lanes 2 and 3). Similar results were obtained when PN day 12 wild-type (+/+) mouse retinal extracts were used (compare lanes 5 and 6). As expected, when retinal extracts from mice lacking AIPL1 (-/-) was used, mAb-AIPL1 does not pull down AIPL1 (lane 8). Purified AIPL1 protein serves as a control (lane 10). IB, immunoblot.

and stabilization of PDE6 subunits by proteasomal inhibitors demonstrate that in the absence of AIPL1, PDE6 subunits are degraded regardless of their normal synthesis.

**AIPL1 Is Essential for Proper Assembly of PDE6 Subunits—**Residual PDE6 present in the retinas lacking AIPL1 are not functional (6). This result suggests that the PDE6 may be misassembled in the absence of AIPL1. Defects in assembly can lead to destabilization of PDE6 subunits observed in the absence of AIPL1. To assess the assembly status of PDE6 subunits, we performed immunoprecipitation using ROS-1 antibody.

ROS-1 is a monoclonal antibody that recognizes rod and cone PDE6 complexes containing both catalytic and inhibitory subunits ( $\alpha\beta\gamma_2$  and  $\alpha'\gamma'_2$ ) (24). A previous study showed that ROS-1 recognizes PDE6 complexes with very high affinity and can deplete 95% of PDE6 activity from bovine retina (24). In agreement with that study, under our IP conditions, we find that ROS-1 is efficient (90%) in recognizing PDE6 heteromer from retinas of wild-type mice (Fig. 4A). However, in the absence of the inhibitory PDE6  $\gamma$  subunit or PDE6  $\beta$  subunit, ROS-1 does not recognize the PDE6 complex (25, 26). Our results also confirm that ROS-1 does not recognize unassembled rod PDE6 present in retinas of *rd* mice, where the PDE6  $\beta$  subunit is missing (Fig. 4, B and C, upper panel). Nevertheless, PDE6 from unaffected cones in *rd* mice can be immunoprecipitated by ROS-1 (Fig. 4C, middle panel). Unlike MOE, ROS-1 antibody does not recognize individually expressed PDE6 subunits in COS-7 tissue culture cells (Fig. 4, D and E, lanes 1–3). Altogether, these results show that ROS-1 recognizes only fully assembled and functional PDE6 complexes.

To test the status of PDE6 assembly, we compared the ability of MOE and ROS-1 to immunoprecipitate PDE6 complexes from wild-type versus AIPL1-deficient retinas. Briefly, after pulse labeling with L-[<sup>35</sup>S]methionine for 1½ h, the amount of assembled PDE6 subunits was assessed by immunoprecipitation with

ROS-1 or MOE antibody. Despite the presence of all three subunits in retina lacking AIPL1 as confirmed by pull-down with MOE antibody, ROS-1 failed to recognize PDE6 subunits from AIPL1-deficient retinas (Fig. 4F, compare lanes 2 and 4). These results suggest that despite the presence of all three PDE6 subunits, they are either not assembled or misassembled in the absence of AIPL1.

To distinguish between these two possibilities, we performed size exclusion chromatography. The hypotonically extracted PDE6 enzyme, from retinas of wild-type and *Aipl1*<sup>-/-</sup> mice at PN day 8, was separated by gel filtration (Superdex 200 10/30 GL). The eluted fractions were analyzed by Western blotting for PDE6 subunits using MOE antibody. The majority of PDE6 was found to be in

the size range of 440 to 290 kDa. Despite reduced levels of PDE6 in retinas lacking AIPL1, an identical separation of PDE6  $\alpha$ ,  $\beta$ , and  $\gamma$  subunits was observed in both wild-type and mice deficient in AIPL1 (Fig. 4G). PDE6 subunits were not detected in void volume, implying that the absence of AIPL1 does not result in aggregation of PDE6 subunits (data not shown). Size exclusion chromatography in conjunction with ROS-1 pull-down suggests that PDE6 subunits in the absence of AIPL1 misassemble and cannot be recognized by ROS-1.

**AIPL1 Interacts with a Catalytic Subunit of Rod PDE6—**It is clear that AIPL1 is needed for proper assembly of the PDE6 heteromer. However, it is not known if AIPL1 interacts with one or all of the subunits of the PDE6 complex.

To investigate the interaction of AIPL1 with PDE6 subunits, we developed a monoclonal antibody that recognizes native AIPL1 from retinal tissues. The specificity of the AIPL1 monoclonal antibody (mAb-AIPL1) was verified by IP using both bovine and mouse retinal extracts. Monoclonal AIPL1 antibody (mAb-AIPL1) immunoprecipitates AIPL1 protein from both mouse and bovine retinal samples (Fig. 5, lanes 2 and 5). The specificity of the antibody was confirmed by the lack of pull-down of the aryl hydrocarbon receptor interacting protein (AIP), a closely related protein that is also expressed in retina (data not shown). Immunoprecipitation of AIPL1 from retinal extracts from adult mice followed by immunoblotting shows that our monoclonal antibody (mAb-AIPL1) is efficient in depleting the majority of AIPL1 (95%). In addition to AIPL1, both catalytic subunits of PDE6 ( $\alpha$  and  $\beta$ ) were specifically found in our IP (Fig. 6, mAb-AIPL1-IP). We also used mass spectrometry to confirm the identity of AIPL1 and catalytic subunits of PDE6 observed in our AIPL1 pull-down (data not shown). We never observed the inhibitory subunit ( $\gamma$ ) of PDE6 co-IP with AIPL1. These results suggest that AIPL1 interacts with the complex of catalytic subunits of PDE6 that excludes the  $\gamma$  subunit (Fig. 6A).

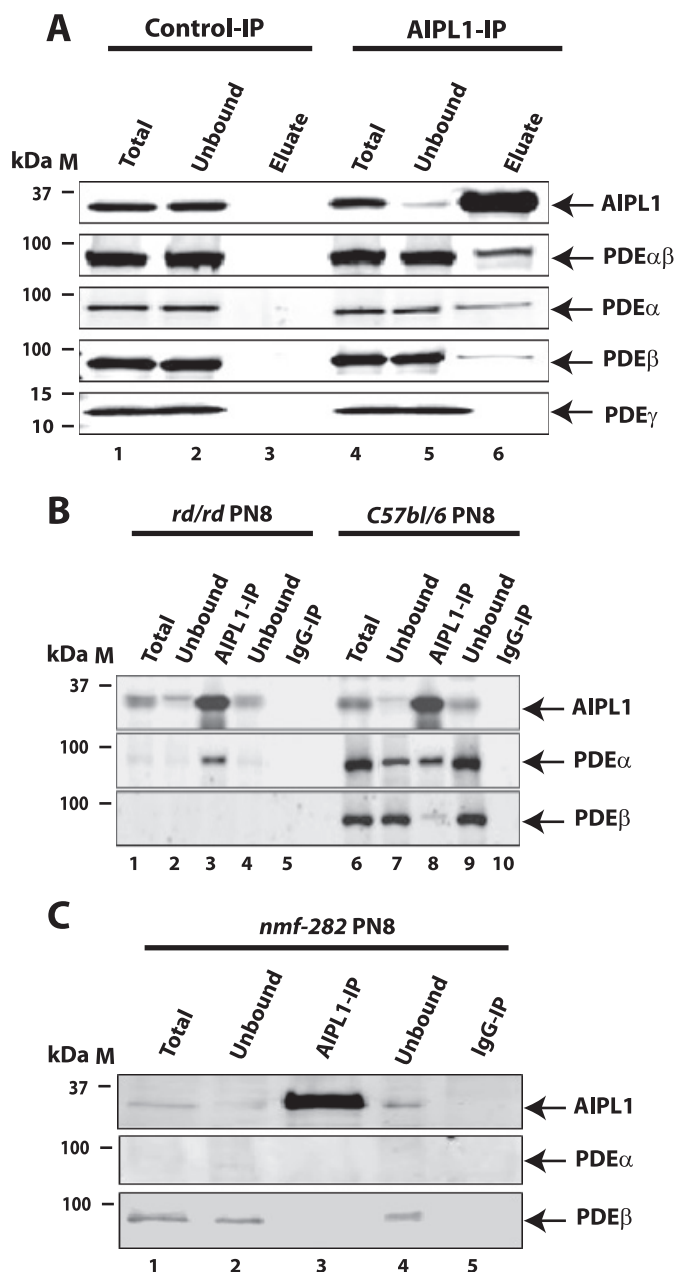


**FIGURE 6. AIPL1 interacts with rod PDE6  $\alpha$  subunit.** *A*, IP with the mAb-AIPL1 column using adult mouse retinal extracts followed by Western blotting with antibodies against the indicated proteins. The mAb-AIPL1 coupled column depletes the majority of AIPL1 from retinal extracts (lanes 4 and 5). 12% of PDE6  $\alpha$  and PDE6  $\beta$  catalytic subunits present were specifically observed in mAb-AIPL1-IP (compare lanes 3 and 6). Control IP was performed using mouse IgG. *B*, IP with the mAb-AIPL1 column using retinal extracts from *rd/rd* mice at PN day 8 lacking the PDE6  $\beta$  subunit show that AIPL1 can interact with 55% of the PDE6  $\alpha$  subunits present (lanes 1–3). In wild-type at PN day 8, AIPL1 associates primarily with 35% of the PDE6  $\alpha$  subunits present (lanes 6–8, lower panel). *C*, IP with the mAb-AIPL1 column using retinal extracts from *nmf-282* mice with defective PDE6  $\alpha$  subunits, show that AIPL1 does not associate with PDE6  $\beta$  in the absence of PDE6  $\alpha$  (lanes 1–3, lower panel). The amount of PDE6  $\alpha$  bound to AIPL1 was calculated based on three independent experiments.

To extend our studies and identify the primary partner of AIPL1, we used *rd* mice that lack the  $\beta$  subunit of PDE6. We used retinal extracts from PN day 8 before the onset of retinal degeneration. In these retinal extracts, mAb-AIPL1 co-immu-

noprecipitates 55% of the PDE6  $\alpha$  subunit (Fig. 6*B*). Lack of PDE6  $\beta$  subunit does not affect the interaction of AIPL1 with the PDE6  $\alpha$  subunit. As a control, we performed a similar IP with AIPL1 antibody in retinal extracts from PN day 8 wild-type mice. We find that AIPL1 interacts primarily with PDE6  $\alpha$  subunits (35%), but a minor amount of PDE6  $\beta$  (8%) was also found (Fig. 6*B*, lanes 3 and 9).

To demonstrate further that AIPL1 interacts with the  $\alpha$  subunit of PDE6, we used retinal extracts from *nmf-282* mice. These mice carry a mutation in PDE6  $\alpha$  (V685M) that severely reduces the PDE6  $\alpha$  levels at PN day 10 (Fig. 6*C*) (27). Under these conditions mAb-AIPL1 does not co-IP with PDE6  $\beta$ . This suggests that AIPL1 does not interact with PDE6  $\beta$  in the absence of PDE6  $\alpha$  (Fig. 6*C*). Altogether, these results show that AIPL1 primarily interacts with the  $\alpha$  subunit of PDE6.

## DISCUSSION

There is a constant need to replenish PDE6 in photoreceptor outer segments in response to phagocytosis of photoreceptor discs. The precise steps involved in synthesis of PDE6 subunits, their assembly in inner segments, and further transport to outer segments of photoreceptor cells is not clear. In addition, catalytic subunits of PDE6 are differentially prenylated, a post-translation modification that is needed for membrane association and that may play a role in assembly of PDE6 subunits (28, 29). Attempts to understand PDE6 biosynthesis and assembly has been severely hampered by the lack of an expression system where functional PDE6 can be produced (29–31). In the absence of a reliable expression system, we used *ex vivo* pulse label, pulse-chase analysis, and IP in retinal tissues from wild-type mice and various mutant mouse models to study the role of AIPL1 in biosynthesis of PDE6. Our findings show that AIPL1 interacts with the catalytic subunit ( $\alpha$ ) of PDE6, and that AIPL1 plays a critical role in the proper assembly of PDE6.

Despite different levels of messages, both PDE6  $\alpha$  and  $\beta$  proteins are present at equimolar ratios in rod photoreceptors (32). This suggests that translation of PDE6  $\alpha$  and PDE6  $\beta$  subunits is regulated and coordinated (32). Even though the mechanism behind this regulation is not understood, it underscores the importance of regulated translation for PDE6 expression. Therefore, we explored the likelihood that reduced PDE6 levels observed in *Aipl1*<sup>-/-</sup> retinas could be caused by a defective translation of PDE6 catalytic subunits. However, we excluded this possibility because our pulse label analysis did not reveal any significant differences in PDE6 synthesis in retinas lacking AIPL1. On the other hand, pulse-chase analysis indicates that all three PDE6 subunits are rapidly degraded in the absence of AIPL1. This degradation of PDE6 can be partially abrogated by addition of proteasomal inhibitors during pulse-chase suggesting that PDE6 subunits are degraded by proteasomes. Collectively, these results suggest that a reduced level of PDE6 in the absence of AIPL1 is caused by rapid turnover due to defective processing of PDE6 subunits. These processing steps include folding, prenylation, and assembly of PDE6 subunits prior to their transport to outer segments of photoreceptors.

Rapid destabilization of rod PDE6 is likely due to lack of assembly or misassembly of PDE6 subunits. Destabilization of PDE6 subunits also is seen in a recently characterized mouse

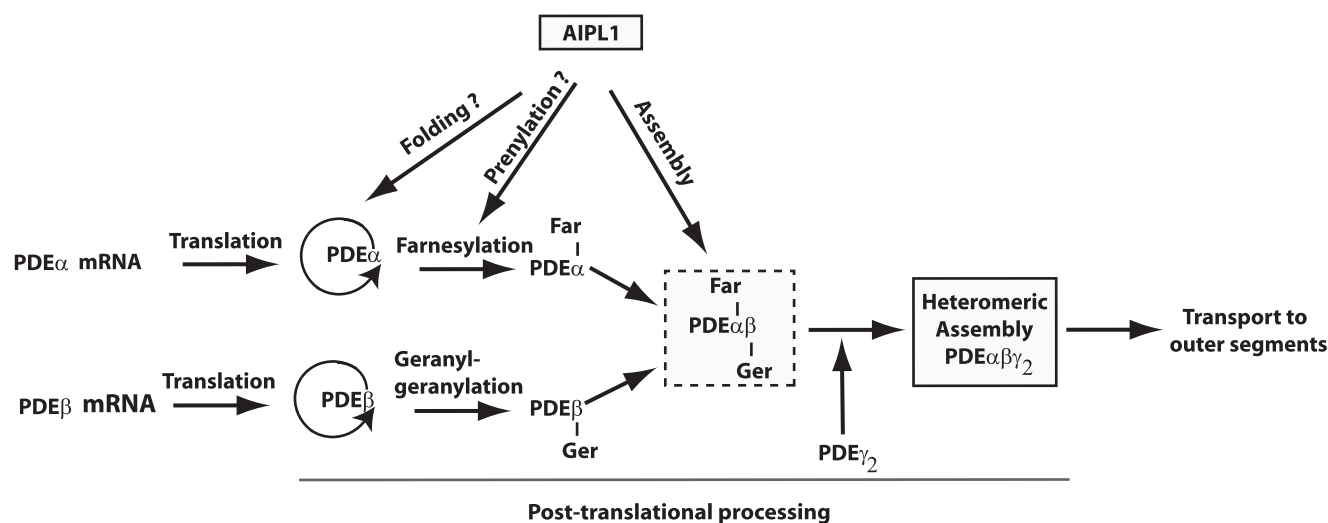


FIGURE 7. **A model depicting the role of AIPL1 in biosynthesis of rod PDE6 heteromer.** AIPL1, a protein essential for stability of PDE6, primarily interacts with the catalytic subunit of rod PDE6  $\alpha$ . Based on our results, we speculate that AIPL1 influences proper assembly and stability of PDE6 subunits through its role in folding and/or prenylation of PDE6 subunits. Folding of PDE6 subunits is denoted by the *curved arrow*. See text for additional details.

model (*nmf-282*) with mutations in PDE6  $\alpha$  leading to reduction in both PDE6  $\alpha$  and  $\beta$  subunits (27). However, the level of the inhibitory subunit (PDE6  $\gamma$ ) is not altered (27). In other mouse models defective in PDE6 subunits, such as in PDE6  $\beta$  (*rd*) or PDE6  $\gamma$  knock-out animals, the levels of their PDE6 partners are not dramatically altered before the onset of retinal degeneration (19, 33). In these mouse models, it is expected that lack of one PDE6 subunit will result in non-assembly of the PDE6 heteromer. However, the non-assembly of PDE6 subunits does not lead to their destabilization. In contrast, changes in AIPL1 dramatically alter the stability of all three subunits of PDE6. In addition, the residual PDE6 present in the absence of AIPL1 is not functional (6). Collectively, these results suggest that in the absence of AIPL1, PDE6 subunits are misassembled. This is in agreement with the results shown in this study. Although PDE6 subunits in the absence of AIPL1 are not functional, our gel filtration analysis suggests that PDE6 subunits in the absence of AIPL1 are present in a complex. However, these PDE6 subunits are not identified by an antibody, ROS-1, that recognizes only the assembled and functional native PDE6 heteromer. This implies that PDE6 in the absence of AIPL1 is misassembled. The misassembled PDE6 complexes are targeted to proteasomes for degradation. This accounts for the severe reduction of PDE6 levels that occur in the absence of AIPL1 (6).

We find that AIPL1 interacts with catalytic subunits of PDE6 in adult retinal tissue. We have confirmed the identities of the interacting partners by mass spectrometry analysis. Under conditions where we can deplete almost 95% or more of AIPL1 using our monoclonal antibody against AIPL1, we were able to co-IP only 12% of total PDE6 present in the cells. This is to be expected, as AIPL1 is present exclusively in the inner segments of photoreceptors, where proteins such as PDE6 are actively synthesized and assembled (4, 9, 22). In contrast, the majority of PDE6 is present in the outer segments, where it is needed for phototransduction. This model is supported by our observation that AIPL1 can interact with 35% of the  $\alpha$  subunit of PDE6 in PN day 8 retina, where outer segment development has not yet taken place.

Our pulldown experiments with adult and PN day 8 retina suggest that AIPL1 interacts with one of the catalytic subunits. To identify the subunit that dominates the PDE6-AIPL1 interaction, we performed pulldowns with retinal extracts from tissues lacking either the  $\alpha$  or  $\beta$  subunit. Our results show that AIPL1 interacts primarily with PDE6  $\alpha$  and is not dependent on PDE6  $\beta$ . We never observed an interaction between AIPL1 and PDE6  $\gamma$  in these studies. These results suggest that AIPL1 is associated with PDE6  $\alpha$  subunits in the inner segments of photoreceptors prior to their interaction with PDE6  $\beta$  and  $\gamma$  subunits.

The pathway for biosynthesis of the PDE6 heteromer is not known. After translation of PDE6 subunits by ribosomes on the endoplasmic reticulum, individual PDE6 subunits are prenylated in the cytosol, then targeted to the endoplasmic reticulum surface for further proteolysis and methylation at their C termini (34). It is not clear if assembly precedes prenylation. We propose that AIPL1 associates with PDE6  $\alpha$  prior to its assembly with  $\beta$  (Fig. 7). The PDE6 inhibitory subunit ( $\gamma$ ) associates with this catalytic subunit intermediate at a later stage, most likely after the extraction of PDE6 from endoplasmic reticulum membranes by PDE  $\delta$  (34–36). The assembled PDE6 heteromers are then transported to outer segments (34). Our results demonstrate that in the absence of AIPL1, PDE6 subunits are not properly assembled. AIPL1 appears to act as a chaperone that induces proper folding of PDE6  $\alpha$  (Fig. 7). This is in agreement with a recent *in vitro* study that demonstrated interaction of AIPL1 with well characterized chaperones, heat shock proteins 70 and 90 (37).<sup>3</sup>

AIPL1 belongs to the immunophilin superfamily, a class of proteins thought to act as molecular chaperones. In the absence of AIPL1, misfolded PDE6 subunits may misassemble. The influence of AIPL1 on rod PDE6 stability may be related to its interaction with the prenylated C termini of PDE6 subunits (Fig. 7). AIPL1 interacts with farnesylated proteins and preny-

<sup>3</sup> S. Koldaivelu and V. Ramamurthy, manuscript in preparation.



lation of rod PDE6 is essential for its stability (22, 29). However, the role of AIPL1 in cones, where PDE6  $\alpha'$  subunits are geranylgeranylated is less clear. A more thorough and direct analysis is needed to assess the prenylation status of PDE6 subunits in the absence of AIPL1. Further studies are required to decipher the mechanisms of complex assembly and transport of functional PDE6 subunits to photoreceptor outer segments. In summary, we have shown that AIPL1 helps to establish proper protein assembly during the early steps of PDE6 synthesis by interacting with the  $\alpha$  subunit of PDE6 prior to its transport to the photoreceptor outer segments.

*Acknowledgments*—We thank Drs. Theodre Wensel, Joseph Beavo, and Cheryl Craft for the generous gift of antibodies. The *nmf-282* mouse model was a kind gift from Dr. Patsy Nishina. We thank Dr. Anand Swaroop for sharing *Nrl* mouse model. We thank Jonathan Linton, Irina Ankoudinova, and members of the Ramamurthy laboratory for help throughout this study.

## REFERENCES

- Dharmaraj, S., Leroy, B. P., Sohocki, M. M., Koenekoop, R. K., Perrault, I., Anwar, K., Khaliq, S., Devi, R. S., Birch, D. G., De Pool, E., Izquierdo, N., Van Maldergem, L., Ismail, M., Payne, A. M., Holder, G. E., Bhattacharya, S. S., Bird, A. C., Kaplan, J., and Maumenee, I. H. (2004) *Arch. Ophthalmol.* **122**, 1029–1037
- den Hollander, A. I., Roepman, R., Koenekoop, R. K., and Cremers, F. P. (2008) *Prog. Retinal Eye Res.* **27**, 391–419
- van der Spuy, J., Munro, P. M., Luthert, P. J., Preising, M. N., Bek, T., Heegaard, S., and Cheetham, M. E. (2005) *Mol. Vis.* **11**, 542–553
- van der Spuy, J., Kim, J. H., Yu, Y. S., Szel, A., Luthert, P. J., Clark, B. J., and Cheetham, M. E. (2003) *Invest. Ophthalmol. Vis. Sci.* **44**, 5396–5403
- Hendrickson, A., Bumsted-O'Brien, K., Natoli, R., Ramamurthy, V., Posin, D., and Provis, J. (2008) *Exp. Eye Res.* **87**, 415–426
- Ramamurthy, V., Niemi, G. A., Reh, T. A., and Hurley, J. B. (2004) *Proc. Natl. Acad. Sci. U.S.A.* **101**, 13897–13902
- Dyer, M. A., Donovan, S. L., Zhang, J., Gray, J., Ortiz, A., Tenney, R., Kong, J., Allikmets, R., and Sohocki, M. M. (2004) *Brain Res. Mol. Brain Res.* **132**, 208–220
- Koenekoop, R. K. (2004) *Surv. Ophthalmol.* **49**, 379–398
- Liu, X., Bulgakov, O. V., Wen, X. H., Woodruff, M. L., Pawlyk, B., Yang, J., Fain, G. L., Sandberg, M. A., Makino, C. L., and Li, T. (2004) *Proc. Natl. Acad. Sci. U.S.A.* **101**, 13903–13908
- Cote, R. H. (2004) *Int. J. Impot. Res.* **16**, Suppl. 1, S28–S33
- Miki, N., Baraban, J. M., Keirns, J. J., Boyce, J. J., and Bitensky, M. W. (1975) *J. Biol. Chem.* **250**, 6320–6327
- Baehr, W., Devlin, M. J., and Applebury, M. L. (1979) *J. Biol. Chem.* **254**, 11669–11677
- Hurley, J. B., and Stryer, L. (1982) *J. Biol. Chem.* **257**, 11094–11099
- Deterre, P., Bigay, J., Forquet, F., Robert, M., and Chabre, M. (1988) *Proc. Natl. Acad. Sci. U.S.A.* **85**, 2424–2428
- Fung, B. K., Young, J. H., Yamane, H. K., and Griswold-Prenner, I. (1990) *Biochemistry* **29**, 2657–2664
- Artemyev, N. O., Surendran, R., Lee, J. C., and Hamm, H. E. (1996) *J. Biol. Chem.* **271**, 25382–25388
- Petersen-Jones, S. M., Entz, D. D., and Sargan, D. R. (1999) *Invest. Ophthalmol. Vis. Sci.* **40**, 1637–1644
- Farber, D. B., Flannery, J. G., and Bowes-Rickman, C. (1994) *Prog. Retinal Eyes Res.* **13**, 31–65
- Tsang, S. H., Gouras, P., Yamashita, C. K., Kjeldbye, H., Fisher, J., Farber, D. B., and Goff, S. P. (1996) *Science* **272**, 1026–1029
- Ausubel, F. M., Brent, R., Kingston, R. E., Moore, D. D., Seidman, J. G., Smith, J. A., and Struhl, K. (2003) *Current Protocols in Molecular Biology*, John Wiley & Sons, Inc., New York
- Makino, C. L., Wen, X. H., Michaud, N., Peshenko, I. V., Pawlyk, B., Brush, R. S., Soloviev, M., Liu, X., Woodruff, M. L., Calvert, P. D., Savchenko, A. B., Anderson, R. E., Fain, G. L., Li, T., Sandberg, M. A., and Dizhoor, A. M. (2006) *Invest. Ophthalmol. Vis. Sci.* **47**, 2185–2194
- Ramamurthy, V., Roberts, M., van den Akker, F., Niemi, G., Reh, T. A., and Hurley, J. B. (2003) *Proc. Natl. Acad. Sci. U.S.A.* **100**, 12630–12635
- van der Spuy, J., Chapple, J. P., Clark, B. J., Luthert, P. J., Sethi, C. S., and Cheetham, M. E. (2002) *Hum. Mol. Genet.* **11**, 823–831
- Hurwitz, R. L., Bunt-Milam, A. H., and Beavo, J. A. (1984) *J. Biol. Chem.* **259**, 8612–8618
- Hurwitz, R. L., and Beavo, J. A. (1984) *Adv. Cyclic Nucleotide Protein Phosphorylation Res.* **17**, 239–248
- Lee, R. H., Lieberman, B. S., Hurwitz, R. L., and Lolley, R. N. (1985) *Invest. Ophthalmol. Vis. Sci.* **26**, 1569–1579
- Sakamoto, K., McCluskey, M., Wensel, T. G., Naggert, J. K., and Nishina, P. M. (2009) *Hum. Mol. Genet.* **18**, 178–192
- Anant, J. S., Ong, O. C., Xie, H. Y., Clarke, S., O'Brien, P. J., and Fung, B. K. (1992) *J. Biol. Chem.* **267**, 687–690
- Qin, N., Pittler, S. J., and Baehr, W. (1992) *J. Biol. Chem.* **267**, 8458–8463
- Muradov, K. G., Granovsky, A. E., and Artemyev, N. O. (2003) *Biochemistry* **42**, 3305–3310
- Muradov, H., Boyd, K. K., and Artemyev, N. O. (2006) *Vision Res.* **46**, 860–868
- Piri, N., Mendoza, E., Shih, J., Yamashita, C. K., Akhmedov, N. B., and Farber, D. B. (2006) *Exp. Eye Res.* **83**, 841–848
- Cunnick, J., and Takemoto, D. J. (1992) *Biochem. Biophys. Res. Commun.* **184**, 461–466
- Karan, S., Zhang, H., Li, S., Frederick, J. M., and Baehr, W. (2008) *Vision Res.* **48**, 442–452
- Norton, A. W., Hosier, S., Terew, J. M., Li, N., Dhingra, A., Vardi, N., Baehr, W., and Cote, R. H. (2005) *J. Biol. Chem.* **280**, 1248–1256
- Zhang, H., Li, S., Doan, T., Rieke, F., Detwiler, P. B., Frederick, J. M., and Baehr, W. (2007) *Proc. Natl. Acad. Sci. U.S.A.* **104**, 8857–8862
- Hidalgo-de-Quintana, J., Evans, R. J., Cheetham, M. E., and van der Spuy, J. (2008) *Invest. Ophthalmol. Vis. Sci.* **49**, 2878–2887
- Campbell, A. M., Burdon, R. H., and van Krippenberg, P. H. (eds) (1984) *Laboratory Techniques in Biochemistry and Molecular Biology: Monoclonal Antibody Technology*, pp. 86–184, Elsevier, New York